



Study on quantitative structure–activity relationship of quaternary ammonium salt collectors for bauxite reverse flotation

Yuehua Hu, Pan Chen, Wei Sun*

School of Minerals Processing and Bioengineering, Central South University, Changsha 410083, China

ARTICLE INFO

Article history:

Received 1 August 2011

Accepted 13 October 2011

Available online 17 November 2011

Keywords:

QSAR

Quaternary ammonium salt

Aluminum-silicate minerals

Kaolinite

Reverse flotation

ABSTRACT

Microflotation tests were performed on such pure minerals as diasporite and kaolinite to detect their respective flotation behaviors and flotation selectivity, in which 20 quaternary ammonium salts were applied as collectors to explore the relationship between the structure and selectivity of quaternary ammonium salt so as to investigate the probability of application of QSAR in the development of flotation reagents. Based on the selection and calculation of quantization parameters, topological parameters and selectivity indices of the reagents, a model with robust predictive abilities was established. The results showed that the shape of molecule, total energy and hydrophobic property were the three major factors affecting the selectivity of collectors. The better matching degree of molecular chain length and molecular configuration and the more negative total energy of the reagent were, the more efficient the reverse flotation separation of aluminum-silicate minerals would be.

© 2011 Elsevier Ltd. All rights reserved.

1. Introduction

Since diasporic-bauxite in China is characterized by high content of aluminum oxide and silica but low mass ratio of aluminum oxide to silica ($A/S = 4\text{--}6$), from which bayer process cannot economically produce aluminum oxide due to the high sodium hydroxide and energy consumption caused by high-silica (Luo et al., 2001; Zhang et al., 2002). Therefore, it is necessary to remove aluminosilicate minerals such as kaolinite to increase the mass ratio of aluminum oxide to silica (Hu et al., 2001; Wang et al., 2003a,b; Zhang et al., 2001). Reverse flotation provides a promising way to remove silicates. As a matter of fact, flotation technology has been extensively applied as a pretreatment prior to bayer process (Hu and Wang, 2004). Recently the cationic amine collectors were considered the most efficient agents and investigated quite intensively (Liu et al., 2009; Zhong et al., 2008; Zhao et al., 2007), which, however, still had their shortcomings such as weak selectivity, low flotation speed and a large amount of foam and so on (Wang et al., 2004; Zhao et al., 2005; Yu et al., 2008; Wang et al., 2003a,b). Thus, bauxite reverse flotation process still has a long way to go before it can be put into commercial use, to which the design and development of high-selectivity collectors for aluminosilicate gangue minerals (mainly kaolinite) are very critical (Chen et al., 2005).

It is known that chemical reactivity and physicochemical properties of organic compounds are decided by their molecular structure.

On the basis of the activity determination of a series of derivatives of the known leading compound, the quantitative-relation that brings out the dependence of a property or activity on entire molecular or its substructural fragment is called quantitative structure–activity relationship (QSAR) (Li, 1992). Since corresponding relations between compounds structure and activity has already been found, QSAR, a successful method of drug development and pharmacological study in medical field, will be very helpful to deepen the understanding of drug mechanism, avoid blindness at work, save manpower, material, resources and money, etc., which has also been extensively used in agricultural chemistry, pharmaceutical chemistry and toxicology (Kar and Roy, 2010; Frid and Matthews, 2010). In minerals processing field, however, this advanced process was researched by only a few scholars (Natarajan and Nirdosh, 2003, 2008). To provide basic data for research in this field and explore cationic collector database, this paper focused on QSAR research of quaternary ammonium salt collector and indicated that collector structure and flotation selectivity were closely linked, which provided new insights into the design and development of novel high efficient collector of reverse flotation for diasporic-bauxite.

2. Materials and methods

2.1. Materials and reagents

Samples of diasporite and kaolinite were obtained from Xiaoyi, Shanxi province of Northern China, which were crushed, hand-selected, and ground in a porcelain mill with agate ball. After being

* Corresponding author. Fax: +86 0731 88830623.

E-mail address: sunmenghu@126.com (W. Sun).

sieved, the -0.074 mm fraction with its purity being above 90% was chosen for microflotation tests. Chemical compositions of diasporite and kaolinite samples were listed in Table 1.

The flotation collectors were divided into three series: single long alkyl chain structure, double long alkyl chain structure and stellate configuration. The first series includes: 0831, 1031, 1231, 1222, 1227, 1431, 1427, 1631, 1622, 1627, 1831; the second includes: D8, D10, D12, D16, D18; and the third: T4, T8, T12, F4. All the collectors were 99.9% analytical reagents purchased from Xiamen Pioneer Technology Co. Ltd. Analytical grade of sodium hydroxide and hydrochloric acid was used for pH control. Details of all reagents were given in Table 2 and Fig. 1.

2.2. Flotation tests

Single mineral flotation tests with diasporite and kaolinite were conducted in a 40 mL flotation cell, each using 3 g of mineral samples in 40 mL of distilled water. After the desired amount of reagents (pH controller or collector) was added, the pulp was agitated for 3 min. Since the pH of suspension was adjusted and the collector was completely dispersed, a 4–5 min flotation period was necessary. The concentrate and tailing samples were filtered, dried, and weighed to calculate the flotation recovery under various flotation conditions.

2.3. Computational methods

All the descriptors were calculated using Gaussian03 (Frisch et al., 2003) and Cerius² 3.0 software. In order to balance the calculation accuracy and calculation time, a smaller basis set was applied to optimize the molecular structure and a larger one was used to calculate the single point energy. Now that a large number of experiments proved that the size of basis set had more impact on the calculation of single point energy than on the structural optimization (Jensen, 2007), in this study, the initial molecular models of reagents were optimized by 3-21G basis set and RHF method, and then the geometries obtained were further optimized and calculated using DFT methods at B3LYP/6-31G (D) level.

3. Results and discussion

3.1. Microflotation tests

The core of using QSAR to screen effective reagents was that all indices must be quantized, analyzed and reflected in a mathematical model. Twenty quaternary ammonium salts were tested as collectors to float the diasporite-bauxite from China. Separation efficiencies of the collectors were taken as the dependent parameter, which was defined as the difference between the % recovery of the valuable mineral and that of the gangue mineral in the float concentrate. For low-grade bauxite the separation efficiency (Es) could be expressed as $Es = \% \text{ kaolinite recovery} - \% \text{ diasporite recovery}$. A larger Es reflected a better reverse flotation separation effect. The quaternary ammonium salts were used in the study, whose effects on the floatability of diasporite and kaolinite at varied pH levels were given in Fig. 2.

Table 1
Chemical analytical results of pure mineral samples/%.

Samples	Grade (mass fraction) (%)									
	Al ₂ O ₃	SiO ₂	Fe ₂ O ₃	TiO ₂	CaO	MgO	K ₂ O	Na ₂ O	H ₂ O	Lost
Kaolinite	39.2	43.67	0.32	1.98	0.01	0.068	0.094	0.028	13.65	13.98
Diasporite	80.98	0.78	0.29	2.84	0.01	0.046	0.007	0.025	14.06	14.5

Table 2
Molecular formula of collectors.

Collectors	Molecular formula
0831	C ₈ H ₁₇ (CH ₃) ₃ NCl
1031	C ₁₀ H ₂₁ (CH ₃) ₃ NCl
1231	C ₁₂ H ₂₅ (CH ₃) ₃ NCl
1222	C ₁₂ H ₂₅ C ₂ H ₅ (CH ₃) ₂ NCl
1227	C ₁₂ H ₂₅ C ₆ H ₅ CH ₃ (CH ₃) ₂ NCl
1431	C ₁₄ H ₂₉ (CH ₃) ₃ NCl
1427	C ₁₄ H ₂₉ C ₆ H ₅ CH ₃ (CH ₃) ₂ NCl
1631	C ₁₆ H ₃₃ (CH ₃) ₃ NCl
1622	C ₁₆ H ₃₃ C ₂ H ₅ (CH ₃) ₂ NCl
1627	C ₁₆ H ₃₃ C ₆ H ₅ CH ₃ (CH ₃) ₂ NCl
1831	C ₁₈ H ₃₇ (CH ₃) ₃ NCl
D8	(C ₈ H ₁₇) ₂ (CH ₃) ₂ NCl
D10	(C ₁₀ H ₂₁) ₂ (CH ₃) ₂ NCl
D12	(C ₁₂ H ₂₅) ₂ (CH ₃) ₂ NCl
D16	(C ₁₆ H ₃₃) ₂ (CH ₃) ₂ NCl
D18	(C ₁₈ H ₃₇) ₂ (CH ₃) ₂ NCl
T4	(C ₄ H ₉) ₃ CH ₃ NCl
T8	(C ₈ H ₁₇) ₃ CH ₃ NCl
T12	(C ₁₂ H ₂₅) ₃ CH ₃ NCl
F4	(C ₄ H ₉) ₄ NCl

For quaternary ammonium salt collectors, the most favorable reagent selectivity could be obtained in acidic condition, which has already been concluded in previous works (Jiang, 2004). Therefore, to facilitate data processing and analysis, this paper focused on the research of selectivity in weak acidic condition (pH from 4 to 6). The recovery of minerals at pH 5 was extracted from flotation curves and shown in Table 3.

Although 11 single long alkyl chain collectors were of similar configuration, different alkyl chain lengths could also lead to a remarkably different flotabilities of diasporite and kaolinite (Fig. 2 and Table 2). The collecting ability of aluminosilicate minerals increased with an increase in alkyl chain length until a maximum (at alkyl chain of 10 carbon atom) was reached, and then declined following the increase of chain length. Compared to the other single alkyl chain collectors, 1031 (10 carbon atoms in straight-chain) showed the strongest collecting ability of kaolinite, while 1627 the weakest; their recovery of kaolinite was 68.55% and 0.34%, respectively. There was a similar law for the other two series of quaternary ammonium salt collectors, in which the optimum alkyl chain length was 8 carbon atoms for double long chain collectors and 4 for stellate collectors.

3.2. Calculation of molecular structure descriptors and establishment of QSAR model

A QSAR model with good predictive abilities relied on the effective transformation of structural details of molecules into numerical quantities. As a molecular metrics, Topological indices (TIs) were extensively used to encode structural details into numbers. Over 300 TIs were illustrated; definitions and calculations thereof could be obtained from the monographs (Devillers and Balaban, 1999; Todeschini and Consonni, 2000). In addition to TIs, quantum mechanical parameters, electronic parameters, physicochemical properties and geometrical parameters that described the molecular surface area and partial atomic charges were also used in

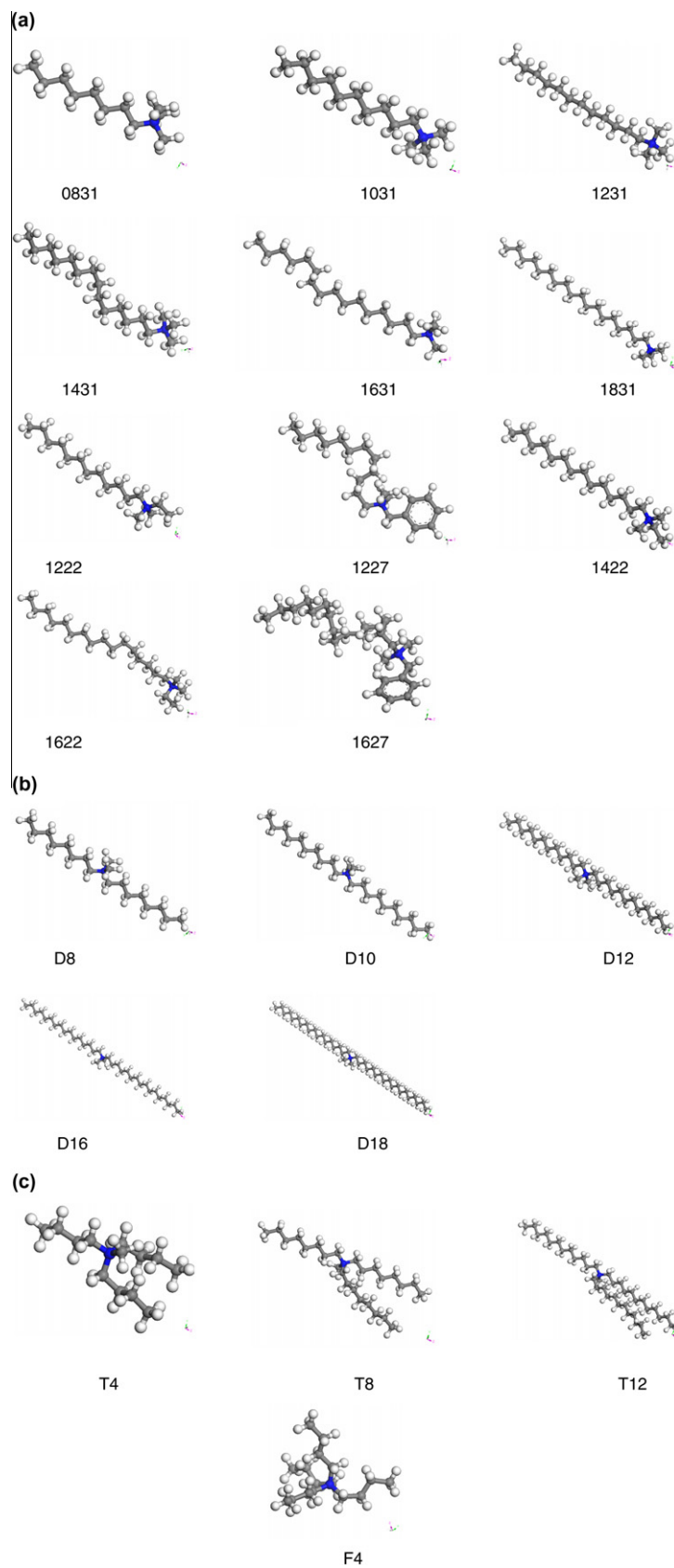


Fig. 1. Cationic structure of collectors (a) single long alkyl chain structure, (b) double long chain structure, and (c) stellate structure (N = blue, C = dark grey, H = white).

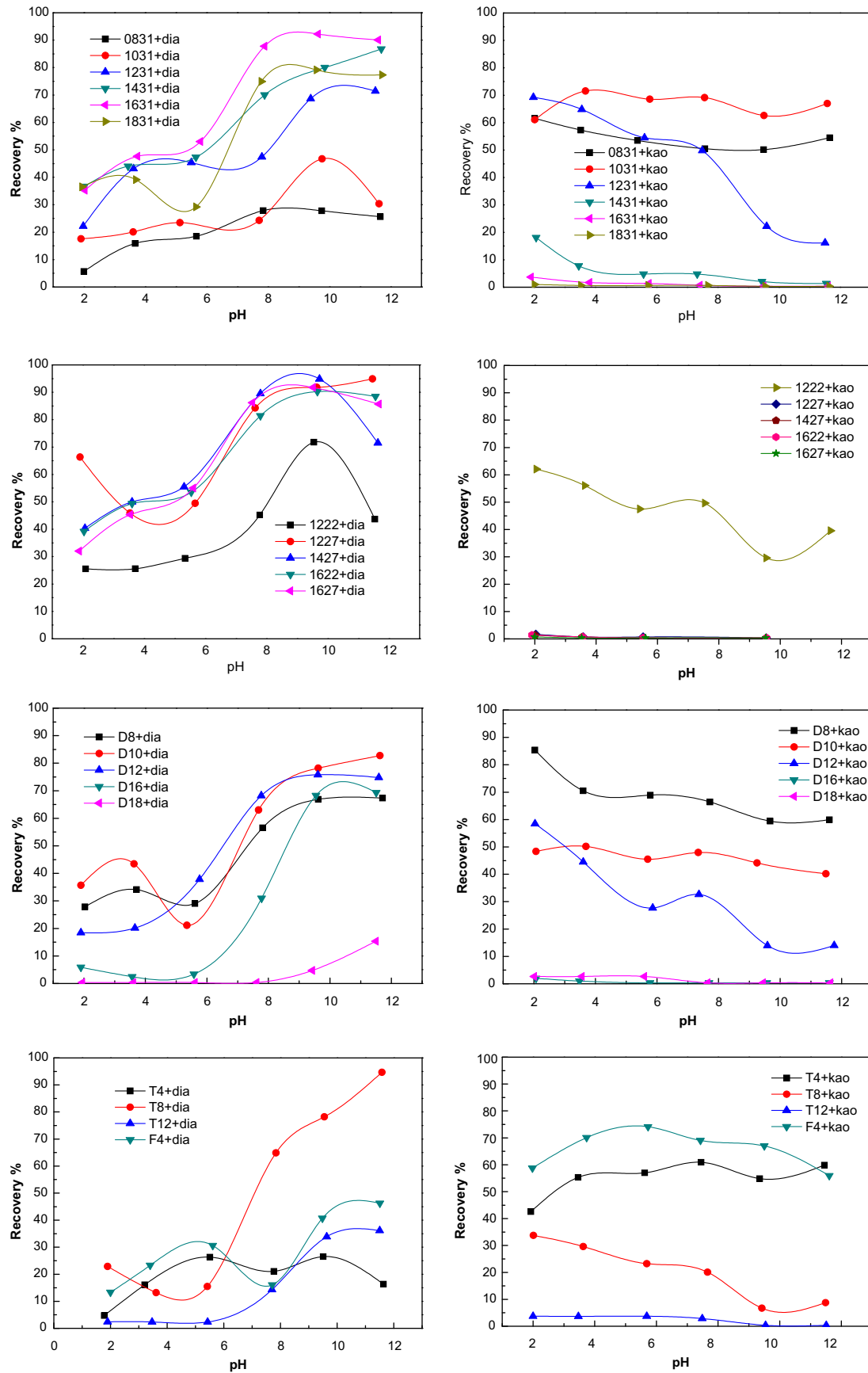


Fig. 2. Flotation recovery of single mineral as a function of pH using 20 collectors (2×10^{-4} mol/L).

Table 3
Results of flotation separation.

Collectors	Recovery of diaspor (%)	Recovery of kaolinite (%)	Es
0831	18.51	53.51	35
1031	23.47	68.55	45.08
1231	45.39	54.51	9.12
1222	29.39	47.47	18.08
1227	49.49	0.67	−48.82
1431	47.33	4.78	−42.55
1427	55.51	0.34	−55.17
1631	53.04	1.36	−51.68
1622	53.51	0.35	−53.16
1627	55.01	0.34	−54.67
1831	29.21	0.67	−28.54
D8	29.02	68.94	39.92
D10	21.14	45.51	24.37
D12	37.84	27.67	−10.17
D16	3.41	0.33	−3.08
D18	0.33	0.33	0
T4	26.35	57	30.65
T8	14.49	23.23	8.74
T12	2.36	3.72	1.36
F4	30.58	74.15	43.57

establishing QSAR models (Karelson et al., 1996; Natarajan and Nirdosh, 2003). Since there were a large number of molecular structure descriptors, the process of effective screen and calculation was a must.

Nine topological indices and six quantum mechanical parameters were screened in this study to describe the characteristics of the external appearance of quaternary ammonium salt collectors, and to indicate the chemical and physical properties of the compound. Definitions of these parameters were listed in Tables 4 and 5.

Statistical program of Cerius² 3.0 was employed to complete statistical analysis. All the twenty quaternary ammonium salts were divided into two kinds: seventeen of them were used as training set to build models (Table 6) and the other three as testing set to test the predictive ability of the models (Table 7).

By using three regression methods, namely, forward stepwise regression, best double regression and best triple regression, three models established were listed below.

For forward stepwise regression:

$$\begin{aligned} \text{Es} &= -13.0436\text{C} - 177.878 \\ \text{rCV}^2 &= -0.211675 \quad R^2 = 0.275345 \quad S = 0.48702 \end{aligned} \quad (\text{M1})$$

For best double regression:

$$\begin{aligned} \text{Es} &= 23.1629\text{R} - 67.3351\text{K} + 169.76 \\ \text{rCV}^2 &= 0.532659 \quad R^2 = 0.579621 \quad S = -0.04696 \end{aligned} \quad (\text{M2})$$

For best triple regression:

$$\begin{aligned} \text{Es} &= -1402.18\text{K} - 15.9617\text{J} + 926.357\text{E} + 3203.13 \\ \text{rCV}^2 &= 0.638714 \quad R^2 = 0.70572 \quad S = 0.067006 \end{aligned} \quad (\text{M3})$$

Table 4
Definitions of six chemical descriptors.

Serial number	Chemical descriptors	Definitions
B	Dipole moment	The product of the positive and negative center distance (r) and the electric center charge (q)
C	HOMO energy	The energy required to remove an electron from the highest occupied molecular orbital
D	LUMO energy	The energy gained when an electron was added to the lowest unoccupied molecular orbital
E	Log P	The octanol–water partition coefficient
I	LUMO density	A measure of the susceptibility of the substrate attacked by an electrophile. It revealed reactive sites based on the distribution of electrons in the lowest unoccupied molecular orbital. Regions of the molecule with high LUMO density had loosely bound electrons that were reactive to electrophilic attack
J	Total energy	The work required to separate the electrons and nuclei infinitely far apart

where capital letters in the equations corresponded to the serial numbers of 15 descriptors, respectively (Tables 4 and 5).

R^2 , rCV^2 and S were the three statistical parameters most frequently used to determine the fitness and predictive abilities of the models (Han, 2007). Specifically, the closer to one R^2 and rCV^2 were and to zero S was, the more robust the model would be. The value of R^2 indicated the quality of fitness, while rCV^2 , to some extent, showed the predictive ability of the model. Generally, 0.6 was regarded as the threshold value for rCV^2 to determine whether the model had a certain predictive ability. Obviously, only model 3 met the predictive requirements, so it had the most powerful goodness of fitness with Es.

The calculated values of Es based on model 3 were presented in Table 8, which indicated that 1631 and 1431 had bigger deviation between the predicted and the experimental values than that of the other 15 reagents. The correlation coefficient could be improved when 1631 and 1431, as abnormal points, were dropped from the regression analyses. The new regression equation was given below:

$$\begin{aligned} \text{Es} &= -1149\text{K} - 12.7828\text{J} + 786.996\text{E} + 2711.79 \\ \text{rCV}^2 &= 0.759816 \quad R^2 = 0.857005 \quad S = 0.097189 \end{aligned} \quad (\text{M4})$$

Coefficient of determination $R^2 = 0.857005$ showed that prediction accuracy of model 4 was 85%. Estimated value of model 4 for Es was shown in Table 9.

Compared with M3, M4 was obviously superior in R^2 and rCV^2 , which indicated that M4 was more credible and stable. Tables 8 and 9 also showed that M4 could provide more accurate estimated values than M3 did.

To further compare the statistical quality of the models, the correlation between experimental and calculated Es values based on model 4 was shown in Fig. 3.

Where x and y denoted calculated and experimental Es values, respectively; error referred to the difference between the average value of y and that of x multiplied with the regression coefficient; R was the linear relativity index; SD was the standard deviation, and P indicated the overall representativeness of the relation. In statistics, the closer to zero error and SD were, the better the fitness of the relations would be. As for R , being closer to one indicated that the linearity of the relations was more significant, while in terms of P , $P < 0.05$ was widely regarded as the threshold for error probability.

In accordance with the statistics of this linear regression equation, the predicted Es and the experimental Es of M4 were in good consistence.

3.3. External validation of QSAR model

QSAR, a successful agent development and pharmacological research method, has been applied in many other fields including medicine, but rarely researched in minerals processing field. What is more, the establishment of high-precision QSAR models requires a lot of data. However, due to the lack of basic database in minerals

Table 5

Definitions of nine topological descriptors.

Serial number	Topological descriptors	Definitions
K	$^0\chi$	Molecular connectivity index of order 0 for the size of the molecule (the number of atoms)
L	$^1\chi$	Molecular connectivity index of order 1 for the degree of star graph likeness
M	$^2\chi$	Molecular connectivity index of order 2 for the degree of linearity
N	$^1\kappa$	Shape index of order 1 for the number of cycles in the chemical sample
O	$^2\kappa$	Shape index of order 2 for the degree of linearity or starlikeness
P	$^3\kappa$	Shape index of order 3 for the degree of branching toward the center
Q	$^0\chi^v$	Valence index of order 0 for the size of the molecule distinguishing non-carbon atoms
R	$^1\chi^v$	Valence index of order 1 for the degree of star graph likeness distinguishing non-carbon atoms
S	$^2\chi^v$	Valence index of order 2 for the degree of linearity distinguishing non-carbon atoms

Table 6

Calculated values of descriptors for training set.

Collectors	Dipole moment (debye)	HOMO energy (eV)	LUMO energy (eV)	Log P	LUMO density	Energy total (hartree)			
0831	28.888	−10.51	−3.093	2.475	−0.046	−489.367			
1231	27.427	−9.506	−3.084	4.06	−0.046	−646.622			
1222	70.723	−9.488	−2.795	4.402	−0.036	−685.937			
1227	22.049	−9.45	−4.021	5.836	0.016	−877.677			
1431	29.253	−9.194	−3.084	4.852	−0.046	−725.249			
1427	30.041	−9.151	−4.022	6.629	0.016	−956.305			
1631	36.123	−8.957	−3.083	5.645	−0.046	−803.876			
1622	33.6	−8.946	−2.796	5.987	−0.036	−843.192			
1627	34.935	−8.919	−4.022	7.422	0.16	−1034.93			
1831	51.386	−8.769	−3.083	6.438	−0.046	−882.504			
D8	7.775	−10.414	−2.639	5.267	−0.043	−764.567			
D10	9.917	−9.863	−2.555	6.852	−0.044	−921.822			
D12	15.558	−9.458	−2.549	8.438	−0.043	−1079.08			
D18	13.501	−8.746	−2.544	13.193	−0.044	−1550.84			
T4	5.692	−12.177	−2.322	3.304	−0.037	−567.995			
T8	11.911	−10.359	−2.184	8.06	−0.034	−1039.76			
F4	3.342	−12.055	−2.343	4.512	−0.023	−685.932			
Collectors	Connectivity index (order 0)	Connectivity index (order 1)	Connectivity index (order 2)	Shape index (order 1)	Shape index (order 2)	Shape index (order 3)	Valence connectivity index (order 0)	Valence connectivity index (order 1)	Valence connectivity index (order 2)
0831	9.45	5.561	5.078	12	6.509	11.111	9.397	5.365	4.782
1231	12.278	7.561	6.493	16	10.173	15.077	12.225	7.365	6.196
1222	12.985	8.121	6.45	17	11.111	12.25	12.932	7.941	6.158
1227	16.098	10.639	8.804	20.045	12.426	11.243	15.319	9.498	7.485
1431	13.692	8.561	7.2	18	12.055	17.067	13.64	8.365	6.903
1427	17.512	11.639	9.511	22.042	14.199	12.964	16.733	10.498	8.192
1631	15.107	9.561	7.907	20	13.959	19.059	15.054	9.365	7.61
1622	15.814	10.121	7.864	21	14.917	16.2	15.761	9.941	7.572
1627	18.927	12.639	10.219	24.038	16	14.72	18.148	11.498	8.899
1831	16.521	10.561	8.614	22	15.879	21.053	16.468	10.365	8.317
D8	14.399	9.121	7.2	19	13.005	14.222	14.347	8.941	6.918
D10	17.228	11.121	8.614	23	16.844	18.182	17.175	10.941	8.333
D12	20.056	13.121	10.028	27	20.727	22.154	20.004	12.941	9.747
D18	28.542	19.121	14.271	39	32.514	34.105	28.489	18.941	13.99
T4	10.864	6.682	5.121	14	8.32	7.04	10.811	6.517	4.851
T8	19.349	12.682	9.364	26	19.753	18.173	19.296	12.517	9.094
F4	12.985	8.243	5.914	17	11.111	7.84	12.932	8.093	5.65

Table 7

Calculated values of descriptors for testing set.

Collectors	Dipole moment (debye)		HOMO energy (eV)		LUMO energy (eV)		Log <i>P</i>	LUMO density	Energy total (hartree)
1031	18.184		−13.492		0.873		3.267	−0.046	−564.001
D16	12.008		−12.412		1.325		11.608	−0.043	−1383.732
T12	26.175		−12.959		1.693		12.815	−0.034	−1500.834
Collectors	Connectivity index (order 0)	Connectivity index (order 1)	Connectivity index (order 2)	Shape index (order 1)	Shape index (order 2)	Shape index (order 3)	Valence connectivity index (order 0)	Valence connectivity index (order 1)	Valence connectivity index (order 2)
1031	10.864	6.561	5.786	14	8.32	13.091	10.811	6.365	5.489
D16	25.713	17.121	12.857	35	28.569	30.118	25.66	16.941	12.575
T12	27.835	18.682	13.607	38	31.527	29.822	27.782	18.517	13.336

Table 8

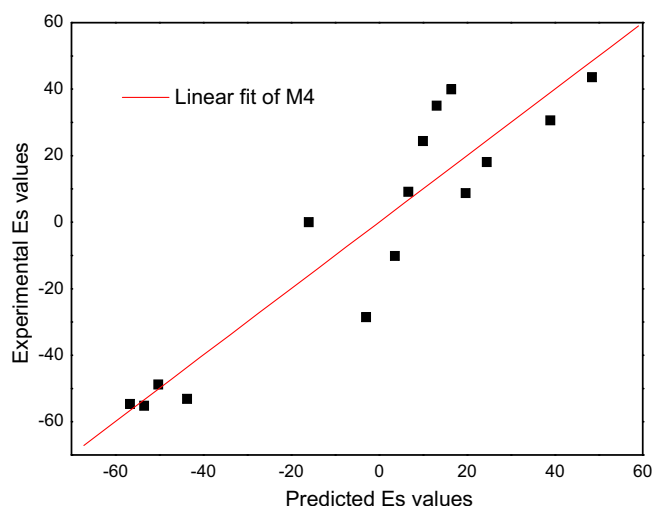
Estimated values of model 3 for selectivity of quaternary ammonium collectors.

Collectors	Recovery of diaspor (%)	Recovery of kaolinite (%)	Separation efficiency (Es)		
			Exp.	Predicted	Residual
0831	18.51	53.51	35	1.494173	33.50583
1231	45.39	54.51	9.12	−3.77912	12.89912
1222	29.39	47.47	18.08	22.18493	4.10493
1227	49.49	0.67	−48.82	−50.6004	1.780377
1431	47.33	4.78	−42.55	−6.41679	36.1332
1427	55.51	0.34	−55.17	−53.2381	1.93195
1631	53.04	1.36	−51.68	−9.05467	42.6253
1622	53.51	0.35	−53.16	−60.2207	7.060681
1627	55.01	0.34	−54.67	−55.876	1.205972
1831	29.21	0.67	−28.54	−11.6927	16.8473
D8	29.02	68.94	39.92	9.429233	30.49077
D10	21.14	45.51	24.37	4.156686	20.21331
D12	37.84	27.67	−10.17	−1.11779	9.05221
D18	0.33	0.33	0	−17	17
T4	26.35	57	30.65	33.07797	2.42797
T8	14.49	23.23	8.74	17.29381	8.55381
F4	30.58	74.15	43.57	45.99436	2.42436

Table 9

Estimated values of model 4 for selectivity of quaternary ammonium collectors.

Collectors	Recovery of diaspor (%)	Recovery of kaolinite (%)	Separation efficiency (Es)		
			Exp.	Predicted	Residual
0831	18.51	53.51	35	13.1022	21.8978
1231	45.39	54.51	9.12	6.680984	2.439016
1222	29.39	47.47	18.08	24.4968	6.4168
1227	49.49	0.67	−48.82	−50.2253	1.405323
1427	55.51	0.34	−55.17	−53.4368	1.73324
1622	53.51	0.35	−53.16	−43.6955	9.46451
1627	55.01	0.34	−54.67	−56.6484	1.978383
1831	29.21	0.67	−28.54	−2.95374	25.5863
D8	29.02	68.94	39.92	16.4451	23.4749
D10	21.14	45.51	24.37	10.02448	14.34552
D12	37.84	27.67	−10.17	3.602316	13.7723
D18	0.33	0.33	0	−16	16
T4	26.35	57	30.65	38.9666	8.3166
T8	14.49	23.23	8.74	19.73155	10.9915
F4	30.58	74.15	43.57	48.49689	4.92689

**Fig. 3.** Fitted curve between predicted value and experimental value $y = 0.99941x + 0.02054$, error = 0.11348, $R = 0.92544$, $SD = 14.40232$, $P < 0.0001$.

processing field, only a few data was extracted to guarantee the basic data for examination of the established models on external validation in this study. Therefore, the detection could only stay on

qualitative level and roughly determine the performance prediction of the models.

The external validation results of QSAR model shown in Table 10 presented good predicted values of D16 and T12, but a large deviation to the predicted value of 1031. There might be two reasons for this: one was the insufficient stability of the model; the other was that the experimental point might be abnormal. Further judgment could not be made due to the limitation of data. Overall, despite its shortcomings, M4, to some extent, could ensure an ideal prediction for most of the data. It was feasible and rational to design quaternary ammonium salt collector of reverse flotation for bauxite using a QSAR model through a follow-up research.

3.4. Mechanism interpretation of QSAR model

In addition to obtaining the predictive results, QSAR modeling could also find the most significant structural factors determining the property of some reagents, which could serve as the direction for designing new collectors and help understand the structure-properties of some reagents.

3.4.1. Significance of parameter of QSAR model

As previously discussed, a three-parameter equation with an interactive correlation coefficient of 0.759816 was obtained for Es as follows.

Table 10

Results of external validation for model 4.

Collectors	Recovery of diaspor (%)	Recovery of kaolinite (%)	Separation efficiency (Es)		
			Exp.	Predicted	Residual
1031	23.47	68.55	45.08	9.681915	35.39809
D16	3.41	0.33	−3.08	−9.02802	5.94802
T12	2.36	3.72	1.36	−0.4104	1.7704

Table 11

Absolute values of descriptors coefficient and mean deviation for model 4.

Descriptors	Absolute value of coefficient	Absolute value of mean deviation	Product
Zeroth order molecular connectivity index	1149	2.751232	3161.165
Total energy	12.7828	175.6704	2245.559
Log <i>P</i>	786.996	1.702007	1339.473

$$Es = -1149K - 12.7828J + 786.996E + 2711.79 \quad (M4)$$

where *K* denoted molecular connectivity index of order 0 for the size of the molecule (the number of atoms); *J* denoted the total energy required to separate the electrons and nuclei infinitely far apart; *E* denoted Log *P* reflecting the hydrophobic property of organics.

Such combination of three descriptors could better predict the selectivity of collectors than others did in this study. Since such important factors as total energy (*J*) and Log *P* (*E*) were widely accepted in the design of flotation reagent, no further explanation was necessary here. As a topological index describing molecular configuration, zeroth order molecular connectivity index was rarely applied in minerals processing field. In addition, this parameter directly influenced the selectivity of quaternary ammonium salt collectors, so it was necessary to make further description.

According to Cerius² 3.0 manual, zeroth order (atoms) molecular connectivity index mainly reflected the size of molecules and atoms, but this could not be easily understood by most minerals processing workers. To obtain a more distinct physical expression, a linear regression analysis was employed. The regression equation of parameter *K* was given below:

$$K = 0.829543L + 0.735002E + 2.97727 \quad (M5)$$

$$rCV^2 = 0.99972 \quad R^2 = 0.999844 \quad S = 0.00012$$

where *K* denoted molecular connectivity index of order 0; *L* denoted molecular connectivity index of order 1 for the degree of star; *E* denoted Log *P* reflecting the hydrophobic property of organics.

M5 showed that parameters *L* and *E* almost completely expressed the characteristics of parameter *K* for an excellent correlation (rCV^2 and R^2 were very close to 1, and *S* was very close to 0). It was assumed accordingly that zeroth order molecular connectivity index was a topology parameter reflecting not only molecular star shaped property but also hydrophobic property. In M5 equation, the positive coefficient for *E* and *L* signified that zeroth order molecular connectivity index decreased (or increased) with the decrease (or increase) of the degree of molecular star shaped property and hydrophobic property.

3.4.2. Mechanism interpretation of QSAR model

According to previous discussion, M4 was the best model established, in which, the negative coefficient for total energy signified that, as previously proved by many researches, its decrease contributed to the improvement of the selectivity. Since the electrostatic force was regarded as the primary force between the collector and silicate, it was generally accepted that the collecting ability of the collector was closely related with its charged properties. In the acidic slurry system, quaternary ammonium salt was

positive ion and kaolinite surface was negatively charged. More negative total energy of reagent ion was conducive to the adsorption of reagent ion on mineral surface via electrostatic interaction.

In the equation, the negative coefficient for zeroth order molecular connectivity index and the positive coefficient for Log *P* denoted that the decrease of zeroth order molecular connectivity index and the increase of Log *P* value were helpful to the improvement of selectivity. Moreover, the equation of M5 showed the increase of Log *P* value would indirectly lead to the increase of zeroth order molecular connectivity index in the same reagent branching degree. Therefore, it is safe to say the best condition could not be obtained by simply increasing hydrophobic chain length of reagent. When hydrophobic chain length changed, the corresponding adjustment of reagent branching structure should also be considered.

There is an optimum region of hydrophobic property for a certain kind of quaternary ammonium salt collector. Hydrophobic property at too low or too high a degree will affect the improvement of reagent selectivity, and the optimum hydrophobic range would change following the change of collector branching degree. This conclusion well correlated with flotation experimental results.

What is more, the model showed further information about which, among the three descriptors, had the most significant influence on the selectivity from the product of absolute value of coefficients and average variations given in Table 11.

As could be seen from Table 11, zeroth order molecular connectivity index was the descriptor having the greatest influence on the selectivity of collectors. Since all three products had the same order

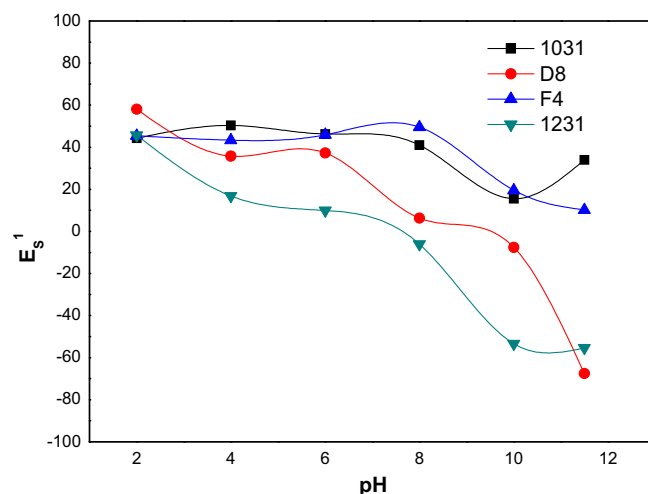


Fig. 4. Effect of pH and 4 collectors (2×10^{-4} mol/L) on the flotation of minerals.

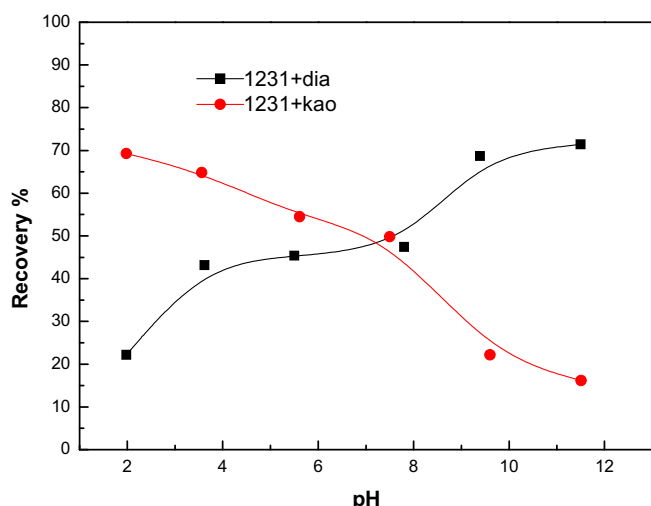


Fig. 5. Recovery of kaolinite and diasporite as a function of pH using 1231 (2×10^{-4} mol/L).

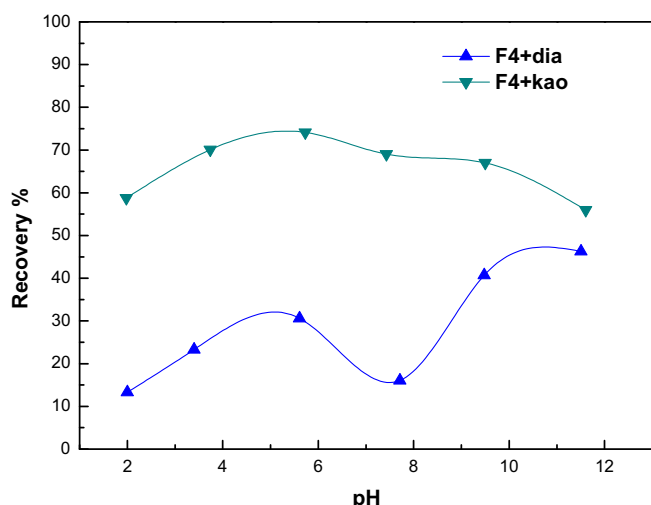


Fig. 6. Recovery of kaolinite and diasporite as a function of pH using F4 (2×10^{-4} mol/L).

of magnitude, it was assumed accordingly that these three parameters played an equal role in the selectivity of collector. Therefore, they should be given equal attention in the design of new reagents.

3.5. Flotation performance of novel quaternary ammonium salt collectors on aluminosilicates

Studies on the separation efficiency (Es) of these quaternary ammonium salt collectors on aluminosilicates were carried out (Fig. 4). In terms of single long alkyl chain, double long alkyl chain and stellate quaternary ammonium salts, 1031, D8 and F4 possessed the best flotation selectivity, compared with traditional collector 1231. Furthermore, stellate quaternary ammonium salt F4 presented optimal flotation performance in a wide pH range.

Figs. 5 and 6 showed the flotation behavior of diasporite and kaolinite using collectors 1231 and F4 respectively. The recovery-pH curves presented that 1231 was unable to realize the reverse flotation separation of two minerals in pH range >6. As expected, F4 was a quite effective cationic collector to separate two minerals even in a weak alkaline pH region.

4. Conclusions

For three structures of quaternary ammonium salt collectors, their primary alkyl chain lengths were closely related to the flotation selectivity. Each reagent structure had an optimal value of primary alkyl length; and too long or too short a chain length would weaken its flotation selectivity.

Nine topological indices and six quantum mechanical parameters of twenty quaternary ammonium salts were calculated. Based on the research of QSAR model, the flotation selectivity of quaternary ammonium salt was determined by its zeroth order molecular connectivity index, total energy and Log P. The more negative the reagent's total energy was, the stronger the reagent's flotation selectivity would be. Moreover, there was an optimal match between primary alkyl chain length and branching structure. The high-efficiency flotation reagent could only be obtained in this region.

The best model was:

$$Es = -1149K - 12.7828J + 786.996E + 2711.79$$

$$rCV^2 = 0.759816 \quad R^2 = 0.857005 \quad S = 0.097189$$

Although there were certain shortcomings, this model provided the ideal prediction for most data. Through a follow-up research, it would be possible to design quaternary ammonium salt collector of reverse flotation for bauxite using a QSAR model, which was a beneficial attempt for the application of QSAR in the fields of design and development of flotation reagent.

Based on the research of QSAR model, three novel quaternary ammonium salt collectors were discovered which were, shown in flotation tests, effective and selective collectors for kaolinite relative to diasporite in a broad pH region, especially F4.

Acknowledgements

This work was supported by the National Key Technology R&D Program for the 11th five-year plan (Grant No. 2008BAB31B02-04-02) and the National Department Public Benefit Research Foundation from Ministry of Land and Resources (Grant No. 201011031), to which the authors express their appreciation.

References

- Chen, X.Q., Hu, Y.H., Wang, Y.H., 2005. Effects of sodium hexametaphosphate on flotation separation of diasporite and kaolinite. *Journal of Central South University of Technology* 12 (4), 420–424.
- Devillers, J., Balaban, A.T., 1999. Topological Indices and Related Descriptors in QSAR and QSPR. Amsterdam, Gordon and Breach.
- Frid, A.A., Matthews, E.J., 2010. Prediction of drug-related cardiac adverse effects in humans-B: use of QSAR programs for early detection of drug-induced cardiac toxicities. *Regulatory Toxicology and Pharmacology* 56 (3), 276–289.
- Frisch, M.J., Trucks, G.W., Schlegel, H.B., 2003. Gaussian03, G03RevB.01. Gaussian, Inc., Pittsburgh PA, USA.
- Han, M., 2007. Probability Statistics. Tongji University, Shanghai, pp. 263–291.
- Hu, Y., Wang, Y., 2004. Flotation Chemistry of Aluminum and Silicate and Desilication of Bauxite. Science Press, Beijing (in Chinese).
- Hu, Y.H., Qiu, G.Z., Miller, J.D., 2001. Aggregation/dispersion of ultrafine silica in flotagent solution. *Transactions of Nonferrous Metals Society of China* 11 (5), 768–773.
- Jensen, F., 2007. Introduction to Computational Chemistry. John Wiley & Sons Ltd, Washington, DC, pp. 233–250.
- Jiang, H., 2004. Studies on Solution Chemistry of Interactions between Cationic Collectors and aluminosilicate Aluminum Minerals in Bauxite Flotation desilica. Changsha, Central South University.
- Kar, S., Roy, K., 2010. QSAR modeling of toxicity of diverse organic chemicals to *Daphnia magna* using 2D and 3D descriptors. *Journal of Hazardous Materials* 177 (1–3), 344–351.
- Karelson, M., Lobanov, V.S., Katritzky, A.R., 1996. Quantum-chemical descriptors in QSAR/QSPR studies. *Chemical Reviews* 96, 1027–1043.
- Li, R.L., 1992. Current situation and outlook of quantitative Structure-activity Relationship. *Medicine Abroad: Pharmacy Section* 19 (6), 321–326.
- Liu, C.M., Hu, Y.H., Cao, X.F., 2009. Substituent effects in kaolinite flotation using dodecyl tertiary amines. *Minerals Engineering* 22 (9–10), 849–852.

- Luo, Z.J., Wang, Y.H., Hu, Y.H., Qiu, G.Z., 2001. Optimization of grinding in reverse flotation for bauxite. *Transactions of Nonferrous Metals Society of China* 11 (3), 444–446.
- Natarajan, R., Nirdosh, I., 2003. Application of topochemical, topostructural, physicochemical and geometrical parameters to model the flotation efficiencies of N-arylhydroxamic acids. *International Journal of Mineral Processing* 71 (1–4), 113–129.
- Natarajan, R., Nirdosh, I., 2008. Quantitative structure–activity relationship (QSAR) approach for the selection of chelating mineral collectors. *Minerals Engineering* 21 (12–14), 1038–1043.
- Todeschini, R., Consonni, V., 2000. Handbook of molecular descriptors. In: Mannhold, R., Kubinyi, H., Timmerman, H. (Eds.), *Methods and Principles in Medicinal Chemistry*, vol. 11. Wiley-VCH, Weinheim, Germany.
- Wang, Y.H., Hu, Y.H., Liu, X.W., 2003a. Flotation de-silicating from diasporic-bauxite with cetyl trimethylammonium bromide. *Journal of Central South University of Technology* 10 (4), 324–328.
- Wang, Y.H., Hu, Y.H., Chen, X.Q., 2003b. Aluminum-silicates flotation with quaternary ammonium salts. *Transactions of Nonferrous Metals Society of China* 7, 715–719.
- Wang, Y.H., Hu, Y.H., He, P.B., 2004. Reverse flotation for removal of silicates from diasporic-bauxite. *Minerals Engineering* 17 (1), 63–68.
- Yu, X.Y., Zhong, H., Liu, G.Y., 2008. Current research status on cationic collector of reverse flotation desilication. *Light Metals* 6, 6–10.
- Zhang, G.F., Feng, Q.M., Lu, Y.P., Liu, G.Y., OU, L.M., 2001. Effect of sodium hexametaphosphate on flotation of bauxite. *Journal of Central South University of Technology: Natural Science* 32 (2), 127–130.
- Zhang, J.F., Hu, Y.H., Wang, D.Z., 2002. Preparation and determination of hydroxamic polyacrylamide. *Journal of Central South University of Technology* 9 (3), 177–180.
- Zhao, S.M., Wang, D.Z., Hu, Y.H., 2005. A series of aminoamides used for flotation of kaolinite. *Journal of University of Science and Technology Beijing* 12 (3), 208–212.
- Zhao, S.G., Zhong, H., Liu, G.Y., 2007. Quaternary ammonium salts collector for flotation of aluminosilicate minerals. *Metal Mine* 2, 45–47.
- Zhong, H., Liu, G.Y., Xia, L.Y., Lu, Y.P., Hu, Y.H., Zhao, S.G., Yu, X.Y., 2008. Flotation separation of diasporic from kaolinite, pyrophyllite and illite using three cationic collectors. *Minerals Engineering* 21, 1055–1061.